Polymer Chemistry

PAPER

View Article Online
View Journal | View Issue

Cite this: *Polym. Chem.*, 2017, **8**, 1714

CO_2-Driven stereochemical inversion of sugars to create thymidine-based polycarbonates by ring-opening polymerisation†

Georgina L. Gregory,[a] Elizabeth M. Hierons,[a] Gabriele Kociok-Köhn,[a] Ram I. Sharma[b] and Antoine Buchard*[a]

The development of biodegradable polymers from renewable resources is vital in addressing the dependence of plastics on petroleum-based feedstocks and growing ocean and landfill waste. Herein, both CO_2 and natural sugar diols are utilised as abundant, safe and renewable building blocks for the synthesis of degradable and biocompatible aliphatic polycarbonates. Despite a strong potential for advanced polymer properties, inspired by Nature's supramolecular base-pairing, polycarbonates from the sugar components of DNA, 2′-deoxyribonucleosides have been limited by the inability of phosgene derivatives to form the cyclic carbonate monomers that would allow for controlled ring-opening polymerisation. CO_2 insertion at 1 atm pressure into methylated thymidine 2′-deoxyribonucleoside, facilitated by organic base 1,8-diazabicyclo-[5.4.0]-undec-7-ene, affected an intramolecular S_N2-like displacement of a tosyl leaving group to yield the cyclic carbonate by stereochemical inversion. Organocatalytic ring-opening polymerisation proceeded rapidly in solution resulting in high monomer conversions of 93% and number-average molecular weights, substantially greater and more controlled than *via* polycondensation routes. The thermodynamic parameters of the polymerisation (ΔH_p = –12.3 ± 0.4 kJ mol^{-1} and ΔS_p = –29 ± 1.1 J mol^{-1} K^{-1}) were determined from the equilibrium monomer conversions over a temperature range of 0 to 80 °C and pseudo-first order kinetics demonstrated. The amorphous thymidine-based polycarbonates exhibited high glass transition temperatures of 156 °C and were found to be highly degradable to the constituent diol under basic aqueous conditions. Static water contact angle measurements and cell studies with MG-63 cell line indicated slightly hydrophilic and biocompatible materials, promising for tissue-engineering applications. The novel, CO_2-driven approach to cyclic carbonate synthesis represents a means of expanding the scope of sugar-based monomers for tailored material properties derived from natural products.

Received 19th January 2017,
Accepted 12th February 2017

DOI: 10.1039/c7py00118e

rsc.li/polymers

Introduction

Reliance on classical petroleum-derived materials and their lack of biodegradability has instigated a drive towards sustainable bio-based polymers from renewable resources.[1] With an ever-growing population, the demand for commodity and engineering plastics is steadily increasing: in 2014, 311 megatonnes of plastics were produced worldwide, a 52% increase since 2002.[2] Readily available sugars are a promising inexpensive renewable alternative to fossil-based feedstocks, owing to their natural origin as well as wide structural and stereochemical diversity.[3] As such synthetic carbohydrate-based materials can give properties comparable to industrial polymers as well as enhanced biodegradability and biocompatibility characteristics, and have the potential to mimic biological materials and functions.[4] For example, the sugar components of DNA, 2′-deoxyribonucleosides are attractive and versatile building blocks, owing to the complementary hydrogen bonding between nucleobase pairs, and have emerged as powerful tools in several fields.[5] Furthermore, the metal coordination chemistry of pyrimidine nucleobases such as thymine (T) opens up the potential for unique polymer applications in metal detection and toxic metal removal.[6] Subsequently, extensive effort has gone into the integration of

[a]*Department of Chemistry, University of Bath, Bath BA2 7AY, UK. E-mail: a.buchard@bath.ac.uk*
[b]*Department of Chemical Engineering, University of Bath, Bath BA2 7AY, UK*

†Electronic supplementary information (ESI) available: Experimental and computational details; spectroscopic and crystallographic data for **1** and **2**; SEC traces, MALDI-ToF spectra, spectroscopic and thermal (TGA, DSC) data for polymers; DFT calculations data and associated digital repositories; tissue engineering protocol and results. CCDC 1523960 and 1523961. For ESI and crystallographic data in CIF or other electronic format see DOI: 10.1039/c7py00118e

nucleobases into the backbone of synthetic polymers[7] or as pendent or terminal groups,[8] either through direct polymerisation or post-synthetic modification.[5b,g,9] Currently, there are several examples, albeit mainly oligomers, of 2′-deoxyribonucleosides bearing carbonate,[10] carbamate,[11] ester,[12] triazole,[13] ether[14] and silyl ether linkages.[15] CO_2 is another abundant, safe and renewable building block and its incorporation into polycarbonates constitutes an important research endeavor within the field of CO_2 utilisation.[16] Moreover, the biodegradability and biocompatibility of aliphatic polycarbonates (APCs) make them a rapidly developing class of polymers for biomedical applications such as tissue engineering scaffolds and drug-delivery carriers.[17] Thus, the construction of functionalised sugar-based APCs in the present work was motivated by the use of these two naturally occurring feedstocks and the creation of novel polymers with desirable properties.

Polycarbonates have been widely prepared by traditional polycondensation with phosgene, phosgene derivatives or dialkyl carbonates.[18] This however overlooks the direct utilisation of CO_2, involves hazardous reagents and often presents challenges in molecular weight control. The copolymerisation of epoxides with CO_2 has been extensively studied as a greener alternative but can be limited by the substrate scope particularly with regards to carbohydrate feedstocks.[19] Enabling larger and well-defined number average molecular weights (M_n) with narrow dispersities ($Đ$), the controlled ring-opening polymerisation (ROP) of typically 6-membered cyclic carbonates has emerged as an attractive choice in polycarbonate production and often proceeds under mild reaction conditions.[20] Both for polymer synthesis and various other applications (*e.g.* battery electrolytes),[21] a growing research effort has focused on the improved synthesis of cyclic carbonates that avoids the use of phosgene or phosgene derivatives and directly incorporates CO_2 (ideally at ambient pressure and temperature).[22]

Currently, sugar-based cyclic carbonates for ROP are limited to those derived from D-glucose,[23] D-mannose[24] and D-xylose[25] (Fig. 1). Cyclocarbonation of *trans*-configured 1,3-diols in 5-membered furanose sugars such as DNA 2′-deoxyribonucleosides has never been achieved to the best of our knowledge. In 1972, Tittensor and Mellish[26] reported the attempted synthesis of the 3′,5′-cyclic carbonate of thymidine and suggested the need for an active ester at the 3′-position rather than 5′-hydroxyl group for cyclisation to occur. Subsequently in 2011, Suzuki *et al.*[10b] selectively placed a carbonyldimidazole (CDI) component at the 3′-position of thymidine and adenosine nucleosides. However, only polycondensation resulted, leading to thymidine-based polycarbonates of low M_n (4700 g mol^{-1}, $Đ$ 1.86).

Herein, the synthesis and successful ROP of a thymidine-based cyclic carbonate incorporating CO_2 at 1 atm pressure is reported. Motivated by the work of Jessop *et al.*,[27] using 1,8-diazabicyclo-[5.4.0]-undec-7-ene (DBU) reagent to capture CO_2 into alcohols, we employ the resulting carbonate as a nucleophile to affect cyclisation *via* an intramolecular S_N2-type reaction. We present DFT calculations that rationalise the monomer synthesis and its ability to be polymerised. The

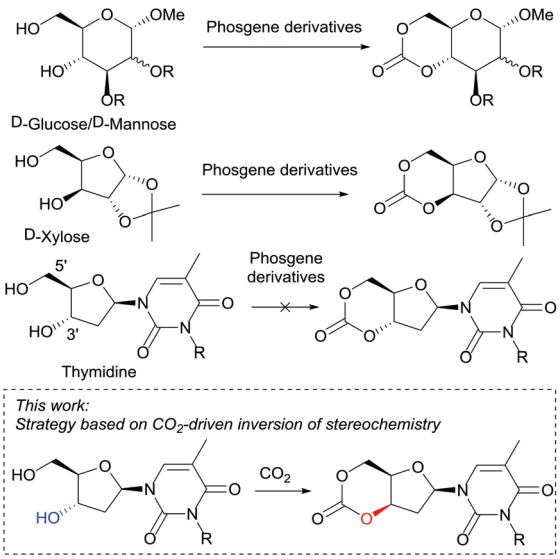

Fig. 1 Unlike D-mannose, D-glucose and D-xylose derived monomers, the cyclic carbonate of thymidine cannot be prepared by traditional routes.

thermodynamic and kinetic parameters of the polymerisation are reported, as well as the resulting new polymer microstructure and thermal properties. A preliminary tissue engineering study is finally presented.

Results and discussion

Monomer synthesis

Synthesis of the *trans*-3′,5′-cyclic carbonate of thymidine using our previously reported method[24] (tosylation of a DBU-introduced carbonate and cyclisation *via* an intramolecular nucleophilic addition-elimination mechanism, leading to stereochemical retention), proved unsuccessful (*trans*-**1**, Fig. 2).

However, DFT calculations[28] of the ring-closing kinetics (transition state $\Delta\Delta G^{\ddagger}$ = +13.3 kcal mol^{-1}) and thermodynamic driving force ($\Delta\Delta G$ = −20.8 kcal mol^{-1}) suggested that this pathway should be accessible at ambient reaction conditions (Scheme S2†). Calculations also indicated that the ring-strain of the hypothetical monomer, consisting of a 6-membered

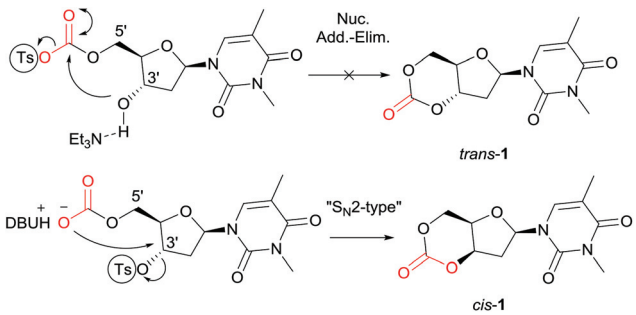

Fig. 2 Synthesis of *cis*-**1** by stereochemical inversion at the 3′-position.

cyclic carbonate *trans*-fused to a furanose sugar ring, was much higher compared to when fused to the 6-membered pyranose ring in reported D-mannose and D-glucose based monomers (Schemes S4 and S5†). For example, ring-opening with methanol is thermodynamically favored with $\Delta\Delta G = -6.7$ kcal mol^{-1} compared to −0.9 and −0.2 kcal mol^{-1} for the mannose and glucose monomers, respectively. The calculated enthalpy of isodesmic ring-opening with dimethyl carbonate ($\Delta\Delta H$) is also 5.5 kcal mol^{-1} more favorable for the *trans*-fused furanose monomer compared to the *trans*-fused D-mannopyranose cyclic carbonate. The pyranose ring can adopt a chair conformation that can accommodate a *trans*-fused ring whereas a furanose-cored monomer may be too highly strained to be isolated (especially in the presence of alcohol). The *cis*-3′,5′-thymidine analogue (*cis*-**1**, Fig. 2) however, lies 9.2 kcal mol^{-1} lower in energy compared to the *trans*- and shows a similar isodesmic ring-strain and in fact greater thermodynamic driving force for ring-opening compared to the D-xylofuranose derived monomer prepared by Gross and co-workers.[25] In that report, cyclocarbonation with ethylchloroformate of the already *cis*-3,5-diol in D-xylose yielded a *cis*-fused cyclic carbonate that successfully underwent ROP. Guided by this insight and further DFT calculations, suggesting favorable cyclisation kinetics and thermodynamics (Scheme S3†), we endeavored to invert the sugar stereochemistry of thymidine and prepare the *cis*-cyclic carbonate by nucleophilic displacement of a tosyl leaving group with a CO_2-generated carbonate.

As shown in Scheme 1, selective tosylation of the 3′-hydroxyl position in thymidine was achieved in good yield by a sequential one-pot silylation followed by tosylation reaction. Subsequent deprotection of the 5′-silyl protecting group was carried out under mild reaction conditions with I_2 in methanol following the procedure outlined by Vaino and Szarek.[29] Unfortunately, protection of the 3-*N* position of the nucleobase was found to be necessary to avoid undesired side reactions during the cyclisation step and potentially during the ROP. Bases such as DBU are known to lead to formation of 2,3′-anhydrothymidine by intramolecular ring-closing of the nucleobase with 3′-leaving groups.[30] As an initial study and proof of concept of the monomer synthesis and ROP potential, the position was methylated in a simple, high yielding step. 3-*N*-Methyl-3′-tosyl-thymidine **2** was then reacted with DBU under 1 atm CO_2 pressure to form a transient amidinium alkyl 5′-carbonate salt, which underwent intramolecular nucleophilic cyclisation with 71% conversion. Subsequent isolation by column chromatography and purification by recrystallisation from toluene gave monomer *cis*-**1** (now referred to as **1** for simplicity), with polymerisation-grade purity, in reasonable yield of 52% (*cf.* 41% for D-xylose, 25–36% for glucose and 57% for mannose-based cyclic carbonates).

The strategy represents a generally applicable method to cyclic carbonate synthesis from natural furanose sugars bearing a *trans*-1,3-diol. It extends the range of sugar-based cyclic carbonate monomers beyond those possible with known sugars and classical reagents such as phosgene and its derivatives, which require a nucleophilic addition-elimination mechanism. Although the need to protect the 3-*N* position of the nucleobase is somewhat limiting, the functionalisation potential of the pyrimidine arm is tremendous, ranging from $Re(CO)_3$ complexes[31] to alkyne functionalities for click chemistry.[5c,32]

As a further demonstration, we also prepared the 3-*N*-benzoyl derivative of **1** (**1-Bz**). Benzoylation could be carried out in tandem with the silylation and tosylation, reducing the number of overall synthetic steps (Scheme S1 and Fig. S12–S14†). Literature precedence has furthermore shown post-polymerisation removal of benzoyl protecting groups.[10b]

The structure of **1** was confirmed by ^{1}H NMR (Fig. 6), ^{13}C{^{1}H} NMR and FTIR spectroscopies as well as electrospray ionisation mass spectrometry (ESI-MS), elemental analysis and single crystal X-ray diffraction. Full NMR assignment was aided by DEPT135, HSQC and COSY experiments (Fig. S1–S5†). In the ^{13}C NMR spectrum, further to the carbonyl environments of the nucleobase, an additional C=O resonance was observed at 147 ppm, typical of a 6-membered cyclic carbonate, and a vicinal $^3J_{3'-4'}$ coupling constant in the ^{1}H NMR spectrum of just 3.9 Hz was consistent with a *cis*-configuration. X-ray analysis of crystals of **1** grown from toluene (Fig. 3)

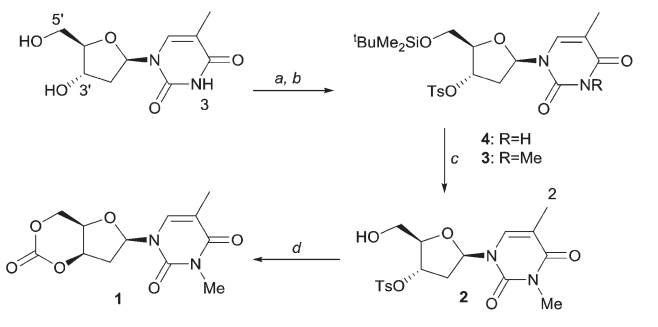

Scheme 1 Synthesis of **1** (a) i: ^{t}BuMe$_2$SiCl, 4-dimethylaminopyridine (DMAP), pyridine, rt, 12 h; ii: TsCl, rt, 24 h, 84%; (b) MeI, K_2CO_3, acetone, 12 h, 93%; (c) 1 wt% I_2 in MeOH, reflux, 2 h, 95%; (d) DBU, CO_2 (1 atm), MeCN, 0–40 °C, 24 h, 52%.

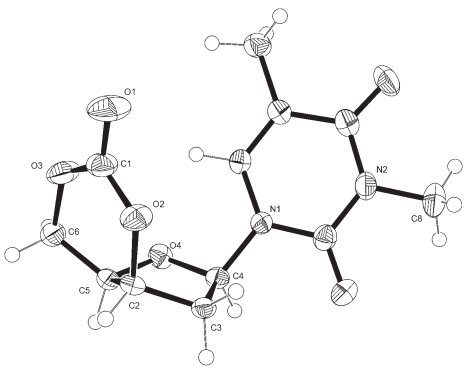

Fig. 3 ORTEP[33] drawing of the crystal structure of 1 with thermal ellipsoids at the 50% probability level (see ESI†). Selected bond lengths (Å) and dihedral angles (°): C(2)–O(2) 1.466 (2), O(2)–C(1) 1.326 (3), O(1)–C(1) 1.202 (3), C(1)–O(3) 1.326 (4), O(3)–C(6) 1.456 (3); C(4)–C(3)–C(2)–C(5) −29.61 (19), C(3)–C(2)–C(5)–O(4) −36.87 (19), C(2)–C(5)–O(4)–C(4) 30.01 (2), C(5)–O(4)–C(4)–C(3) 10.5 (2), O(4)–C(4)–C(3)–C(2) 12.6 (2).

further corroborated stereochemical inversion at the 3′-carbon to form the 3′,5′-*cis*-cyclic carbonate in which the furanose ring adopts a strained 4′-*endo*-3′-*exo* twist ($^4T_3$) conformation. This is likely retained in solution as the ring-methylene H-2′ protons display very different chemical shifts and *J*-coupling constants consistent with the Karplus equation. In contrast the unconstrained furanose ring in the preceding *trans*-3′,5′-diol **2** adopts a 2-*endo* (^{2}E) envelope conformation (see crystal structure in ESI†).

Ring-opening polymerisation (ROP)

The ROP of **1** was initially explored with bifunctional organocatalyst, 1,5,7-triazabicyclo[4.4.0]dec-5-ene (TBD) and 4-methyl benzyl alcohol initiator. Polymerisation proceeded rapidly at 25 °C in CH_2Cl_2, reaching a plateau at 80% monomer conversion (determined by ^{1}H NMR spectroscopy) after 1 h for a monomer-to-initiator feed ratio of 100 and 1 mol L^{-1} initial monomer concentration, $[M]_0$. Further addition of monomer after 24 h led to establishment of a new equilibrium monomer conversion indicating no catalyst deactivation and a concentration dependent equilibrium polymerisation. A higher monomer conversion of 90% was achieved at a higher $[M]_0$ of 2.5 mol L^{-1} (Fig. 4).

A linear kinetic plot is consistent with pseudo-first order kinetics, typical for ROP, from which a k_{app} of 1.39 ± 0.005 h^{-1} was determined (inset Fig. 4 and S15†). The high melting point of the monomer (204–205 °C) and low thermal stability (178–205 °C, 88% mass loss, T_{inf} 248 °C) prevented polymerisations from being carried out in the melt. The temperature dependence of the equilibrium polymerization was also investigated at fixed $[M]_0$, catalyst loading and initiator concentration in 1,2-dichloroethane solvent to access a wider temperature range of 0–80 °C. A plot of $\ln[M]_{eq}$ *versus* the reciprocal

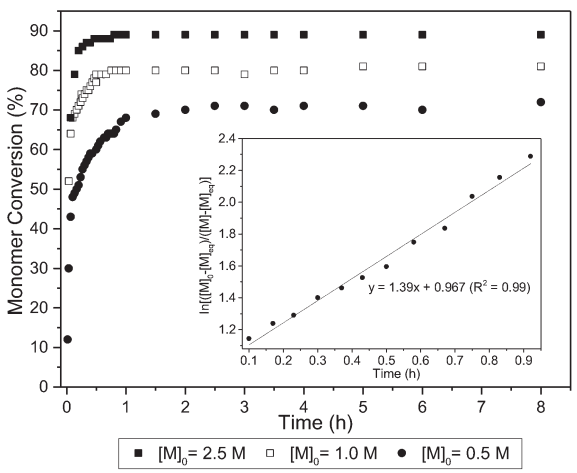

Fig. 4 ROP of **1** with 4-MeBnOH and TBD catalyst: conversion *versus* time for different $[M]_0$. Carried out at 25 °C in CH_2Cl_2 for $[M]_0 : [TBD]_0 : [4\text{-MeBnOH}]_0$ ratio of 100 : 1 : 1. Monomer conversion was determined by ^{1}H NMR spectroscopy by relative integration of the anomeric H-1′ proton. (inset) Kinetic plot carried out under the same conditions for $[M]_0$ = 0.5 mol L^{-1}.

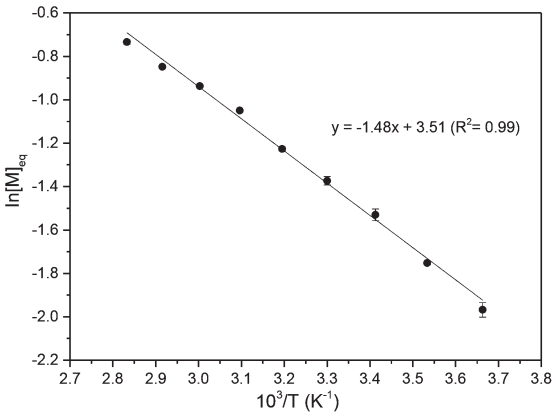

Fig. 5 ROP of **1** with 4-MeBnOH and TBD catalyst: calculation of the thermodynamic parameters from a plot of $\ln[M]_{eq}$ as a function of 1/*T*, where *T* is the absolute temperature. Carried out in 1,2-dichloroethane, over a temperature range of 0–80 °C for $[M]_0$ = 0.5 mol L^{-1} and $[M]_0 : [TBD]_0 : [4\text{-MeBnOH}]_0$ = 100 : 1 : 1. Polymerisations were repeated three times at each temperature and an average taken.

of the absolute temperature gave an estimate of the polymerisation thermodynamic parameters (Fig. 5): ΔH_p = −12.3 ± 0.4 kJ mol^{-1} and ΔS_p = −29 ± 1.1 J mol^{-1} K^{-1}. For comparison, Endo and co-workers[34] reported an enthalpic driving force of −26.4 kJ mol^{-1} for the anionic polymerisation in THF of unsubstituted trimethylene carbonate and accompanying −44.8 J mol^{-1} K^{-1} entropy decrease ($[M]_0$ = 1 mol L^{-1}). A decrease in ΔH_p with increased steric bulk of substituted derivatives was attributed to distortion of the polymer backbone as opposed to a conformational effect on the monomer. Interestingly, for polymer recyclability, the polymerisation mixture at 0 °C, which showed a 72% conversion to polymer at equilibrium, resulted in near quantitative recovery of the monomer upon heating to 80 °C.

A linear increase in M_n with percentage monomer conversion whilst maintaining narrow dispersities indicated that the polymerisation proceeded in a controlled fashion up to 60% monomer conversion (Fig. 6). Initially excellent agreement was observed between the calculated M_n and those estimated by size exclusion chromatography (SEC) *versus* polystyrene standards with $CHCl_3$ eluent. For example, the polymer at 54% monomer conversion had a M_n of 7210 g mol^{-1} ($Đ$ 1.12) as estimated by SEC (Fig. S17†), only slightly lower than the predicted[35] 7740 g mol^{-1}. Once the thermodynamic equilibrium was reached and with longer reaction times, a broadening of the polymer distribution was observed due to transesterification reactions.

Matrix-assisted laser desorption/ionisation time-of-flight (MALDI-ToF) mass spectrometry of this polymer showed a major linear polymer series of M_n 7120 g mol^{-1} and expected 4-methyl benzyl alcohol and O–H end groups (Fig. 7 and S19†). A minor (19%) cyclic species with *m*/*z* consistent with no end-groups and an integer number of repeat units (*m*/*z* ~282.25), was also observed due to backbiting of the polymer chain. As the polymer chain grows and monomer concen-

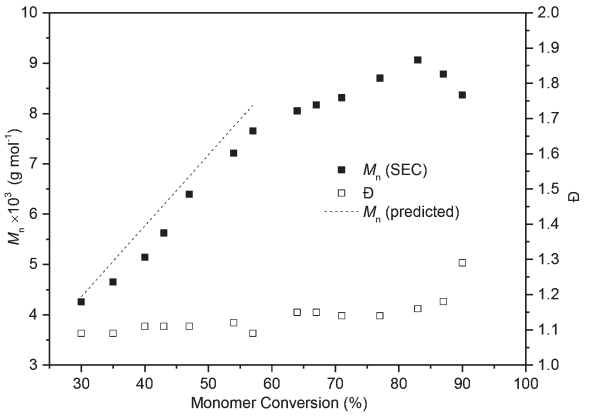

Fig. 6 Plot of M_n and $Đ$ *versus* monomer conversion for a polymerisation carried out at 0 °C with $[M]_0$ = 2.5 mol L^{-1} and 50 : 1 : 1 $[M]_0$: $[TBD]_0$: $[I]_0$. Conversion was determined by ^{1}H NMR spectroscopy of aliquots quenched with excess benzoic acid. M_n and $Đ$ were estimated by SEC *versus* polystyrene standards using a refractive index (RI) detector and $CHCl_3$ eluent.

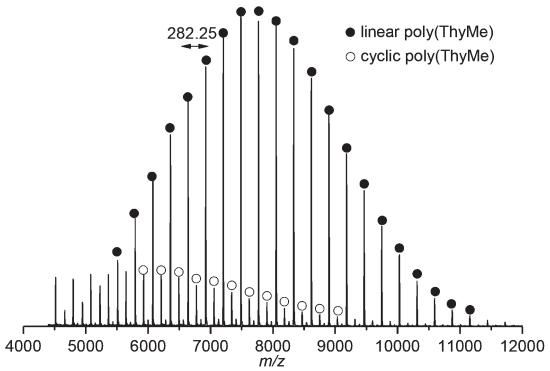

Fig. 7 MALDI-ToF mass spectrum of polymer ($M_{n,SEC}$ 7210 g mol^{-1}, $Đ$ 1.12) showing major linear and minor cyclic polymeric species (distribution assigned based on molecular masses and corresponding formulas, see Fig. S19† for details).

tration decreases, a greater rate of chain backbiting relative to chain propagation may account for deviations observed between the calculated and SEC estimated M_n at higher monomer conversions. Dilution of the reaction conditions to 0.5 mol L^{-1} in an attempt to favour macrocycle formation resulted in lower M_n (Table 1, entry 1) and in more cyclic species observed by MALDI-ToF analysis (Fig. S21†). The lack of chain end in macrocycles should prevent reversion of the polymer to the monomer at elevated temperatures, however, difficulty in separating the cyclic and linear species prevented us from rigorously investigating the issue. Polymeric macrocycles are also interesting in their own right, including those derived from nucleosides, *e.g.* as supramolecular complexes with metal coordination characteristics.[12]

The largest molecular weights, up to 17 000 g mol^{-1} ($Đ$ 1.3) were achieved at 0 °C and $[M]_0$ of 2.5 mol L^{-1} (Table 1, entry 2). A greater disparity between the theoretical M_n and those determined by SEC was observed at higher $[M]_0/[I]_0$ ratios, most likely due to chain back-biting reactions. To explore the influence of the catalytic system on the control of M_n, metal complexes were tested for the ROP of **1**. $Sn(Oct)_2$ catalyst with 4-MeBnOH initiator at 120 °C in toluene did not yield homopolymer. $Y(O^iPr)_3$ or $Al(OTf)_3$ with BnOH initiator resulted in no control with only low M_n (1800–3910 g mol^{-1}, $Đ$ 1.35–1.39) in DCM, dioxane and toluene solvents at 0, 25, 70 and 120 °C. Although highly active for lactide ROP in CH_2Cl_2 at rt, the zinc(II) alkoxide catalyst (L1ZnOEt) reported by Williams *et al.*[36] was slower compared to TBD for the ROP of **1**, as was the (BDI-1)ZnEt catalyst[37] with 4-MeBnOH initiator (Table 1, entries 3 and 4).

Polycarbonate properties

Initial insight into the structure of the thymidine-based polycarbonates was gained by NMR spectroscopy. Shown in Fig. 8, coalescence of the H-5′ and H-4′ proton environments in the ^{1}H NMR spectrum of the polymer compared to the monomer

Table 1 ROP of 1[a]

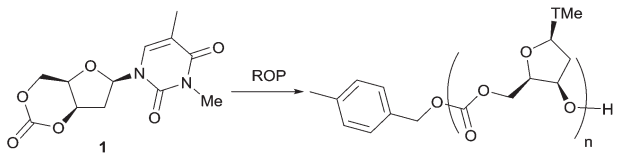

Entry	Temp. (°C)	Cat.	$[M]_0 : [C]_0 : [I]_0$	Conv.[b] (%)	Time (h)	M_n[c] [Đ]
1[d]	0	TBD	100 : 1 : 1	68	4	4260 [1.09]
2	0	TBD	150 : 1 : 1	90	3	17 000 [1.30]
3[e]	25	L1ZnOEt	100 : 1	71	20	7250 [1.22]
4[f]	25	(BDI-1)				
ZnEt	100 : 1 : 1	60	24	5240 [1.15]		
5	25	TBD	100 : 1 : 1	90	3	11 000 [1.27]
6	0	TBD	100 : 1 : 1	93	3	15 400 [1.28]

[a] All polymerisations were carried out at $[M]_0$ = 2.5 mol L^{-1} in CH_2Cl_2 unless stated otherwise. [b] Determined by ^{1}H NMR spectroscopy in $CDCl_3$. [c] g mol^{-1}, calculated by SEC with $CHCl_3$ eluent *versus* polystyrene standards (RI detector). [d] $[M]_0$ = 0.25 mol L^{-1}. [e] L1 = 2,4-di-*tert*-butyl-6-{[(2′-dimethylaminoethyl)methylamino]-methyl}phenolate. [f] BDI-1 = 2-((2,6-diisopropylphenyl)amido)-4-((2,6-diisopropylphenyl)-imino)-2-pentene.

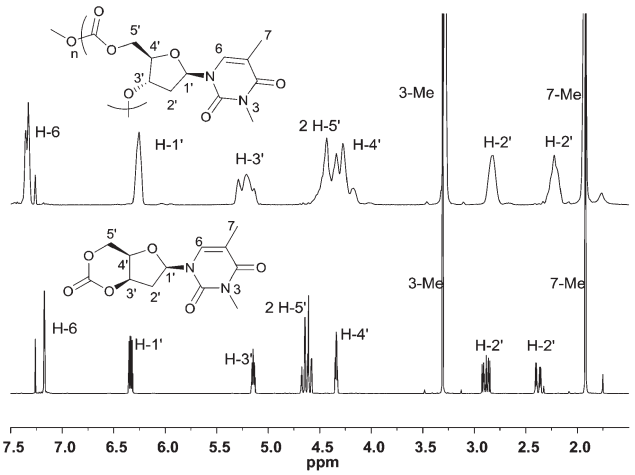

Fig. 8 Comparison of the ^{1}H NMR spectra (400 MHz, $CDCl_3$) of monomer **1** (bottom) and its polymer (top, Table 1, entry 6).

was consistent with loss of constraint upon ring-opening of the cyclic carbonate moiety. In addition, retention of the distinct chemical environments of the furanose ring 2′-methylene protons suggest that the sugar may adopt a similar puckered conformation in the polymer backbone to that observed in the monomer. $^{13}C\{^{1}H\}$ NMR analysis revealed three carbonate environments centered at 154.4, 153.6 and 152.8 ppm, consistent with tail–tail, head–tail and head–head linkages that would arise from the cleavage at either side of the asymmetric carbonate by either a free secondary or primary propagating alcohol chain. Relative assignments were suggested based on previous work,[23a,24,25] and by the 1 : 2 : 1 integration ratio observed, which further suggested a regiorandom propagation of the chain (Fig. S9†). Further splitting observed within these three distinct environments is attributed to long range sequence effects as also reported for regiorandom glucose[23a] and xylose[25] derived polycarbonates. DFT calculations[28] of the initiation step in the ROP of **1** with 4-MeBnOH and TBD catalyst support this lack of preference for ring-opening to expose either a free primary ($\Delta\Delta G$ = −5.6 kcal mol^{-1}) or secondary hydroxyl group ($\Delta\Delta G$ = −6.6 kcal mol^{-1}) for chain propagation (Fig. S38†).

The thermal properties of the polycarbonates were investigated by thermogravimetric analysis (TGA) and differential scanning calorimetry (DSC). The onset of thermal degradation occurred at relatively low temperatures of ∼170 °C, reaching a maximum rate of mass loss (T_{inf}) around 246 °C for polymers of M_n 11 000 and 15 400 g mol^{-1} (Table 1, entries 5 and 6). High mass losses of 91 and 94%, respectively were achieved by ∼300 °C (Fig. S22†). Analysis of the gases evolved by tandem mass spectrometry confirmed the presence of *m*/*z* 44 attributed to the loss of CO_2^+ (Fig. S24†). The polymers exhibited high glass transition temperatures (Fig. S25–S27†); a T_g of 156 °C was measured for polycarbonate of M_n 15 400 g mol^{-1} and is attributed to restricted rotation about the furanose ring backbone and to the bulky thymine group. For comparison, furanose-cored and isopropylidene-protected D-xylose polycarbonate exhibited a T_g of 128 °C (for M_n = 13 200 g mol^{-1}).[25] Pyranose backboned polycarbonates derived from isopropylidene-protected D-mannose and methyl protected D-glucose showed T_g of 152 °C (13 600 g mol^{-1})[23] and 122 °C (14 700 g mol^{-1}),[24] respectively. No transitions associated with a melting domain were observed implying an amorphous polymer, which was further confirmed by powder X-ray diffraction (Fig. S28†).

The hydrolytic stability of the water insoluble polymer was investigated at 0.25 wt% at rt in water, 1 mol L^{-1} HCl and 1 mol L^{-1} NaOH, as well as in PBS buffer at 37 °C in presence of *Candida antartica* lipase B. After 1 week, no dissolution or loss of mass by SEC was observed in the case of water and 1 mol L^{-1} HCl. NMR analysis of the supernatant in D_2O revealed no environments. Under the alkali conditions, the polymer was observed to dissolve after 4 hours. ^{1}H NMR spectroscopy in D_2O after 24 h at 4 wt% revealed proton environments consistent with the *cis*-diol of 3-*N*-methyl thymidine (Fig. S29 and S30†). Mass spectrometry (HR-MS ESI) after 24 h further confirmed the presence of the diol suggesting complete hydrolytic degradation of the polymer to its constitute components. In the case of lipase B, unknown degradation products were detected in solution after one week. Static water contact angle measurements of polymer thin films drop cast onto glass slides revealed an average contact angle of 48 ± 1°. This was more hydrophobic than the monomer but less hydrophilic compared to the glass control (Fig. S32†).

Cell attachment studies were carried out with a human osteoblast cancer cell line, MG-63, on polymer films drop cast onto glass slides. Cell attachment after a 1 h incubation period (37 °C, 5% CO_2) was comparable to the empty tissue culture polystyrene well-plate and glass controls, and indicated the possibility of thymidine-based materials to support cells (Fig. S33–S35†). After a longer 24 h incubation period, cell attachment dropped compared to the empty well-plate control suggesting further modifications to the polymer surface are required for it to serve as an effective tissue engineering scaffold. Nevertheless, the choice of the 3-*N* protecting group and general applicability of the strategy present wide-scope and future opportunities for novel biomaterials with applications in the tissue engineering and regenerative medicine fields. Other degradable polymers attractive in this area, such as PLA and PLGA, are notoriously difficult to functionalise.[38] Therefore, the successful preliminary ROP of benzoyl-protected monomer (**1-Bz**, see ESI†) offers promise for more elaborate functionality as well as post-polymerisation modifications, including self-assembly with base-paired nucleoside polycarbonates.

Conclusions

In summary, a novel strategy for the synthesis of challenging sugar-based cyclic carbonate monomers is presented that utilises CO_2 as a C1 resource at 1 atm pressure. Sugar-based

resources previously inaccessible for ROP such as 2′-deoxyribonucleosides can thus be efficiently converted to cyclic carbonate monomer. Here, novel polycarbonates derived from thymidine are reported. DBU-facilitated CO_2 insertion into the 5′-hydroxyl group of 3-*N*-protected thymidine 2′-deoxyribonucleoside sugar introduces a carbonate nucleophile to affect an intramolecular displacement of a 3′-tosyl leaving group, resulting in stereochemical inversion. The isolated *cis*-configured 3′,5′-cyclic carbonate undergoes ROP under mild reaction conditions with organocatalyst TBD and 4-MeBnOH alcohol initiator to yield novel thymidine-based polycarbonates. The kinetic and thermodynamic parameters of the equilibrium polymerisation were established and MALDI-ToF MS revealed thymidine-based polycarbonates with both linear and cyclic topologies. Thermal analysis revealed high glass transition temperatures and a low onset of thermal degradation. Static water contact angle measurements were carried out and cell attachment studies with MG-63 cell line indicated promising biocompatible materials. Work is ongoing to explore the functionalisation of the 3-*N* position of the thymine nucleobase to impart specific properties for targeted applications.

Acknowledgements

The EPSRC (EP/N022793/1; EP/L016354/1/CDT in Sustainable Chemical Technologies, studentship to GLG), Roger and Sue Whorrod (fellowship to AB) and the Royal Society (RG/150538) are acknowledged for research funding. We thank the University of Bath HPC for computing resources.

Notes and references

1 (*a*) A. Gandini, T. M. Lacerda, A. J. F. Carvalho and E. Trovatti, *Chem. Rev.*, 2015, **116**, 1637–1669; (*b*) C. K. Williams and M. A. Hillmyer, *Polym. Rev.*, 2008, **48**, 1–10; (*c*) A. Llevot, P.-K. Dannecker, M. von Czapiewski, L. C. Over, Z. Söyler and M. A. R. Meier, *Chem. – Eur. J.*, 2016, **22**, 11510–11521; (*d*) A. Gandini and T. M. Lacerda, *Prog. Polym. Sci.*, 2015, **48**, 1–39; (*e*) A. Pellis, E. Herrero Acero, L. Gardossi, V. Ferrario and G. M. Guebitz, *Polym. Int.*, 2016, **65**, 861–871; (*f*) M. J. L. Tschan, E. Brule, P. Haquette and C. M. Thomas, *Polym. Chem.*, 2012, **3**, 836–851; (*g*) T. Iwata, *Angew. Chem., Int. Ed.*, 2015, **54**, 2–8.

2 http://www.plasticseurope.org/information-centre/publications.aspx, (accessed 08/12/2016).

3 (*a*) J. A. Galbis, M. d. G. García-Martín, M. V. de Paz and E. Galbis, *Chem. Rev.*, 2015, **116**, 1600–1636; (*b*) J. A. Galbis and M. G. García-Martín, *Top. Curr. Chem.*, 2010, **295**, 147–176; (*c*) J. A. Galbis and M. G. García-Martín, in *Monomers, Polymers and Composites from Renewable Resources*, ed. M. N. Belgacem and A. Gandini, Elsevier, Oxford, 2008, pp. 89–114; (*d*) *Biobased Monomers, Polymers, and Materials*, ed. P. B. Smith and R. A. Gross, American Chemical Society, 2012; (*e*) Y. Tokiwa and M. Kitagawa, in *Polymer Biocatalysis and Biomaterials II*, American Chemical Society, 2008, vol. 999, pp. 379–410; (*f*) G. L. Gregory, E. M. Lopez-Vidal and A. Buchard, *Chem. Commun.*, 2017, **53**, 2198–2217.

4 (*a*) A. S. Carlini, L. Adamiak and N. C. Gianneschi, *Macromolecules*, 2016, **49**, 4379–4394; (*b*) N. G. Ricapito, C. Ghobril, H. Zhang, M. W. Grinstaff and D. Putnam, *Chem. Rev.*, 2016, **116**, 2664–2704.

5 (*a*) J. Shelton, X. Lu, J. A. Hollenbaugh, J. H. Cho, F. Amblard and R. F. Schinazi, *Chem. Rev.*, 2016, **116**, 14379–14455; (*b*) R. McHale and R. K. O'Reilly, *Macromolecules*, 2012, **45**, 7665–7675; (*c*) A. H. El-Sagheer and T. Brown, *Chem. Soc. Rev.*, 2010, **39**, 1388–1405; (*d*) S. Cheng, M. Zhang, N. Dixit, R. B. Moore and T. E. Long, *Macromolecules*, 2012, **45**, 805–812; (*e*) A. Poma, H. Brahmbhatt, J. K. Watts and N. W. Turner, *Macromolecules*, 2014, **47**, 6322–6330; (*f*) P. K. Lo and H. F. Sleiman, *J. Am. Chem. Soc.*, 2009, **131**, 4182–4183; (*g*) H. Kuang, S. Wu, Z. Xie, F. Meng, X. Jing and Y. Huang, *Biomacromolecules*, 2012, **13**, 3004–3012.

6 (*a*) B. Lippert and P. J. Sanz Miguel, *Acc. Chem. Res.*, 2016, **49**, 1537–1545; (*b*) C. Xing, H. Yuan, S. Xu, H. An, R. Niu and Y. Zhan, *ACS Appl. Mater. Interfaces*, 2014, **6**, 9601–9607.

7 G. S. Collier, L. A. Brown, E. S. Boone, B. K. Long and S. M. Kilbey, *ACS Macro Lett.*, 2016, **5**, 682–687.

8 A. S. Karikari, B. D. Mather and T. E. Long, *Biomacromolecules*, 2007, **8**, 302–308.

9 (*a*) I. H. Lin, C.-C. Cheng, C.-W. Huang, M.-C. Liang, J.-K. Chen, F.-H. Ko, C.-W. Chu, C.-F. Huang and F.-C. Chang, *RSC Adv.*, 2013, **3**, 12598–12603; (*b*) B. D. Mather, M. B. Baker, F. L. Beyer, M. A. G. Berg, M. D. Green and T. E. Long, *Macromolecules*, 2007, **40**, 6834–6845; (*c*) A. Jatsch, A. Kopyshev, E. Mena-Osteritz and P. Bäuerle, *Org. Lett.*, 2008, **10**, 961–964; (*d*) I. H. Lin, C.-C. Cheng, Y.-C. Yen and F.-C. Chang, *Macromolecules*, 2010, **43**, 1245–1252; (*e*) H. J. Spijker, F. L. van Delft and J. C. M. van Hest, *Macromolecules*, 2007, **40**, 12–18.

10 (*a*) J. R. Tittensor, *J. Chem. Soc. C*, 1971, 2656–2662; (*b*) M. Suzuki, T. Sekido, S.-i. Matsuoka and K. Takagi, *Biomacromolecules*, 2011, **12**, 1449–1459.

11 J. M. Coull, D. V. Carlson and H. L. Weith, *Tetrahedron Lett.*, 1987, **28**, 745–748.

12 N. Calcerrada-Muñoz, I. O'Neil and R. Cosstick, *Nucleosides, Nucleotides Nucleic Acids*, 2001, **20**, 1347–1350.

13 H. Isobe, T. Fujino, N. Yamazaki, M. Guillot-Nieckowski and E. Nakamura, *Org. Lett.*, 2008, **10**, 3729–3732.

14 J. Sengupta and A. Bhattacharjya, *J. Org. Chem.*, 2008, **73**, 6860–6863.

15 K. K. Ogilvie and J. F. Cormier, *Tetrahedron Lett.*, 1985, **26**, 4159–4162.

16 (*a*) W. N. R. Wan Isahak, Z. A. Che Ramli, M. W. Mohamed Hisham and M. A. Yarmo, *Renewable Sustainable Energy Rev.*, 2015, **47**, 93–106; (*b*) A. Dibenedetto, A. Angelini and P. Stufano, *J. Chem. Technol. Biotechnol.*, 2014, **89**, 334–353; (*c*) M. Aresta, A. Dibenedetto and A. Angelini, *Chem. Rev.*, 2014, **114**, 1709–1742; (*d*) Y. Qin, X. Sheng, S. Liu, G. Ren,

X. Wang and F. Wang, *J. CO2 Util.*, 2015, **11**, 3–9; (*e*) M. Aresta and A. Dibenedetto, *Dalton Trans.*, 2007, 2975–2992; (*f*) S. M. Guillaume and L. Mespouille, *J. Appl. Polym. Sci.*, 2014, **131**, 40081.

17 (*a*) S. Tempelaar, L. Mespouille, O. Coulembier, P. Dubois and A. P. Dove, *Chem. Soc. Rev.*, 2013, **42**, 1312–1336; (*b*) J. Xu, E. Feng and J. Song, *J. Appl. Polym. Sci.*, 2014, **131**, 39822–39838; (*c*) J. Feng, R.-X. Zhuo and X.-Z. Zhang, *Prog. Polym. Sci.*, 2012, **37**, 211–236.

18 E. Leino, P. Mäki-Arvela, V. Eta, D. Y. Murzin, T. Salmi and J. P. Mikkola, *Appl. Catal., A*, 2010, **383**, 1–13.

19 M. R. Kember, A. Buchard and C. K. Williams, *Chem. Commun.*, 2011, **47**, 141–163.

20 G. Rokicki and P. G. Parzuchowski, in *Polymer Science: A Comprehensive Reference*, ed. K. Matyjaszewski and M. Möller, Elsevier, Amsterdam, 2012, pp. 247–308.

21 S. A. Freunberger, Y. Chen, Z. Peng, J. M. Griffin, L. J. Hardwick, F. Bardé, P. Novák and P. G. Bruce, *J. Am. Chem. Soc.*, 2011, **133**, 8040–8047.

22 (*a*) M. Honda, M. Tamura, K. Nakao, K. Suzuki, Y. Nakagawa and K. Tomishige, *ACS Catal.*, 2014, 1893–1896; (*b*) M. Honda, M. Tamura, Y. Nakagawa and K. Tomishige, *Catal. Sci. Technol.*, 2014, **4**, 2830–2845; (*c*) F. D. Bobbink, W. Gruszka, M. Hulla, S. Das and P. J. Dyson, *Chem. Commun.*, 2016, **52**, 10787–10790.

23 (*a*) K. Mikami, A. T. Lonnecker, T. P. Gustafson, N. F. Zinnel, P. J. Pai, D. H. Russell and K. L. Wooley, *J. Am. Chem. Soc.*, 2013, **135**, 6826–6829; (*b*) R. Kumar, W. Gao and R. A. Gross, *Macromolecules*, 2002, **35**, 6835–6844; (*c*) O. Haba, H. Tomizuka and T. Endo, *Macromolecules*, 2005, **38**, 3562–3563.

24 G. L. Gregory, L. M. Jenisch, B. Charles, G. Kociok-Köhn and A. Buchard, *Macromolecules*, 2016, **49**, 7165–7169.

25 Y. Shen, X. Chen and R. A. Gross, *Macromolecules*, 1999, **32**, 2799–2802.

26 J. R. Tittensor and P. Mellish, *Carbohydr. Res.*, 1972, **25**, 531–534.

27 P. G. Jessop, D. J. Heldebrant, X. Li, C. A. Eckert and C. L. Liotta, *Nature*, 2005, **436**, 1102–1102.

28 DFT calculations of the ring-closing kinetics and thermodynamics were carried out using the following protocol: ωB97XD/6-31+g(d)/SCRF=(cpcm,solvent=acetonitrile) at a temperature of 298 K. The protocol includes an dispersion term shown to reproduce reaction barriers effectively. DFT calculations of monomer ring-strain were carried out the ωB97XD/6-311++g(2d,p)/SCRF=(cpcm,solvent=dichloromethane)/298 K level of theory. DFT computations of the initiation step in the ROP of 1 were carrried at the following level of theory: rωB97XD/6-311+g(d,p)/6-31+g(d)/cpcm=dichloromethane/298 K.

29 A. R. Vaino and W. A. Szarek, *Chem. Commun.*, 1996, 2351–2352.

30 W. Hua, C. Changmei, Z. Hongchao, L. Xiaohong, F. Chang, X. Shanshan and Z. Yufen, *Chem. Lett.*, 2005, **34**, 432–433.

31 M. D. Bartholoma, A. R. Vortherms, S. Hillier, J. Joyal, J. Babich, R. P. Doyle and J. Zubieta, *Dalton Trans.*, 2011, **40**, 6216–6225.

32 K. Liu, L. Zheng, Q. Liu, J. W. de Vries, J. Y. Gerasimov and A. Herrmann, *J. Am. Chem. Soc.*, 2014, **136**, 14255–14262.

33 L. J. Farrugia, *J. Appl. Crystallogr.*, 2012, **45**, 849–854.

34 J. Matsuo, K. Aoki, F. Sanda and T. Endo, *Macromolecules*, 1998, **31**, 4432–4438.

35 Calculated as M_r(4-MeBnOH) + (M_r(**1**) × [**1**]$_0$/[4-MeBnOH]$_0$ × conv./100%).

36 C. K. Williams, L. E. Breyfogle, S. K. Choi, W. Nam, V. G. Young, M. A. Hillmyer and W. B. Tolman, *J. Am. Chem. Soc.*, 2003, **125**, 11350–11359.

37 (*a*) B. M. Chamberlain, M. Cheng, D. R. Moore, T. M. Ovitt, E. B. Lobkovsky and G. W. Coates, *J. Am. Chem. Soc.*, 2001, **123**, 3229–3238; (*b*) M. Cheng, A. B. Attygalle, E. B. Lobkovsky and G. W. Coates, *J. Am. Chem. Soc.*, 1999, **121**, 11583–11584.

38 G. L. Fiore, F. Jing, J. V. G. Young, C. J. Cramer and M. A. Hillmyer, *Polym. Chem.*, 2010, **1**, 870–877.